

Analytical Methods

Accepted Manuscript



This is an *Accepted Manuscript*, which has been through the Royal Society of Chemistry peer review process and has been accepted for publication.

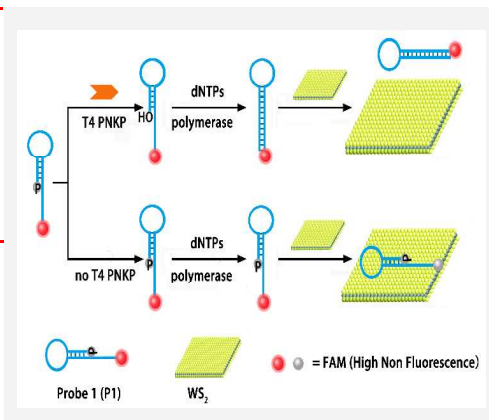
Accepted Manuscripts are published online shortly after acceptance, before technical editing, formatting and proof reading. Using this free service, authors can make their results available to the community, in citable form, before we publish the edited article. We will replace this *Accepted Manuscript* with the edited and formatted *Advance Article* as soon as it is available.

You can find more information about *Accepted Manuscripts* in the [Information for Authors](#).

Please note that technical editing may introduce minor changes to the text and/or graphics, which may alter content. The journal's standard [Terms & Conditions](#) and the [Ethical guidelines](#) still apply. In no event shall the Royal Society of Chemistry be held responsible for any errors or omissions in this *Accepted Manuscript* or any consequences arising from the use of any information it contains.

Development of a highly sensitive sensing platform for T4 polynucleotide kinase phosphatase and its inhibitors based on WS₂ nanosheet

Xiaomeng Liu, Jia Ge, Xiangyu Wang, Zhan Wu, Guoli Shen, Ruqin Yu**



a novel strategy for simply and sensitivity nucleotide kinase phosphatase activity assay based on WS₂ nanosheets.

1
2
3
4
5
6
7
8
9
10
11
12
13
14
15
16
17
18
19
20
21
22
23
24
25
26
27
28
29
30
31
32
33
34
35
36
37
38
39
40
41
42
43
44
45
46
47
48
49
50
51
52
53
54
55
56
57
58
59
60

Cite this: DOI: 10.1039/c0xx00000x

www.rsc.org/xxxxxx

ARTICLE

Development of a highly sensitive sensing platform for T4 polynucleotide kinase phosphatase and its inhibitors based on WS₂ nanosheet

Xiaomeng Liu, Jia Ge, Xiangyu Wang, Zhan Wu*, Guoli Shen, Ruqin Yu*

Received (in XXX, XXX) Xth XXXXXXXXX 20XX, Accepted Xth XXXXXXXXX 20XX

DOI: 10.1039/b000000x

Dephosphorylation of the 3' termini of nucleic acids, catalyzed by various repair enzymes is important for cellular events, such as DNA replication, recombination. Here, using T4 polynucleotide kinase phosphatase (T4 PNKP) as a model target, a novel fluorescence nanosensor based on the FRET between dye labelled DNA and WS₂ nanosheets has been developed for monitoring the activity and inhibition of T4 PNKP. In this assay, we designed a single-strand dye labelled probe that formed self-complementary structure at one end and with a 3'-phosphoryl end that served as the substrate for T4 PNKP. Once the phosphorylated probe was hydrolyzed by T4 PNKP, the resulting probe with a 3'-hydroxyl end was immediately elongated to form double-strand product by Klenow fragment polymerase (KF polymerase). WS₂ nanosheets was introduced to quench the fluorescence of the single-strand dye labelled probe without polymerase elongation. The dye labelled double-strand product preserves most of the fluorescence when mixed with WS₂ nanosheets. Because of the super quenching ability and the high specific surface area of WS₂ nanosheets, the as-proposed platform exhibits an excellent performance with wide linear range and low detection limit. Additionally, the effect of its inhibitors has also been investigated. The method not only provides a universal platform for monitoring activity and inhibition of DNA 3'-phosphatases but also shows great potential in biological process researches, drug discovery, and clinic diagnostics.

Introduction

DNA terminated with a 3'-phosphate is a common product of DNA damage resulting from exposure to both external genotoxic agents and endogenous sources of stress, which can be mutagenic and detrimental to survival.¹⁻² It is required to remove the 3'-phosphate restoring the 3'-termini to hydroxyl form to make the reestablishment of the continuity of DNA strand possible by the DNA polymerization and ligation events.³⁻⁵ Dephosphorylation of the 3' phosphate is usually catalyzed by various repair enzymes, which include the commonly used T4 polynucleotide kinase phosphatase (PNKP). T4 PNKP first discovered in 1965 has the capacity to phosphorylate DNA at 5'-hydroxyl by catalyzing the transfer of the γ -phosphate residue of ATP to nucleic acids and oligonucleotides, and it can act as a DNA 3'-phosphatase.⁶ Acceptable substrates include double-stranded and single-stranded DNA, RNA, and individual 3'-phosphate nucleotide bases. T4 PNKP plays an important role in detection of DNA adducts or oligonucleotides, nucleic acid metabolism, and repair of DNA lesions.⁷⁻¹⁰ Considering its important role in RNA and DNA repair, sensitive and selective detection of T4 PNKP is of great importance.

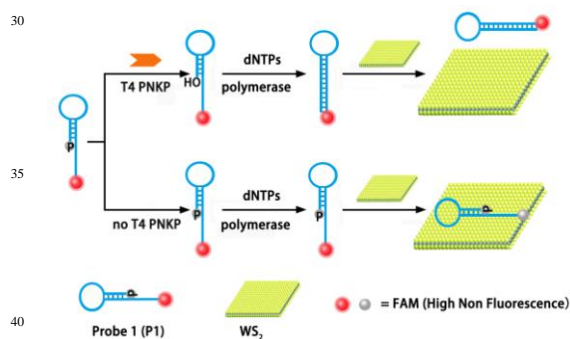
There have been several methods for the detection of dephosphorylation and the assay of activity of T4 PNKP,

including radioisotope ³²P-labeling, polyacrylamide gel electrophoresis (PAGE), autoradiography and fluorescence.¹¹⁻¹⁴ However, these methods have the shortcomings of being time consuming, laborious, not sensitive, or requiring the radiolabeling of substrates. Therefore, alternative assay methods circumventing the afore-mentioned problems need to be explored for the investigation of the dephosphorylation of nucleic acids. Ma *et al* described a fluorescence assay using molecular beacon DNA probes to investigate the dephosphorylation process of nucleic acids by T4 PNKP.¹⁵ However, design of specific dye labelled molecular beacon DNA is difficult and costly. Thus, the development of more sensitive and convenient methods for T4 PNKP assay is still required.

Two-dimensional nanomaterials have received much attention in recent years owing to their unusual quantum properties and surface effect. Graphene is a successful example of 2D carbon material, exhibiting exceptional physical properties such as a high electron conductivity and excellent mechanical strength.¹⁶ Hence, graphene has attracted significant research interest and hold great potential for many applications.¹⁷⁻²¹ WS₂ nanosheets are archetypical examples of inorganic analogues of graphene, the layer of a WS₂ is three atoms thick with the composition of hexagonal layer of metal atoms W sandwiched between two layers of chalcogen atoms.^{22, 23} Compared with graphene, WS₂

nanosheets can be synthesized in large scale, and can be directly dispersed in aqueous solution, implying that WS₂ nanosheets will hold great promise as a novel nanomaterial for biomedical applications. Nevertheless, the use of WS₂ nanosheets as a bioanalytical platform has not widely explored. In addition, most transition-metal ions possess intrinsic fluorescence quenching properties.²⁴ It has been reported that graphene oxide (GO) can bind and quench dye-labelled single-stranded DNA probes, while it has less affinity toward double-stranded DNA or secondary and tertiary structured single-stranded DNA.^{20, 25} We for the first time found that WS₂ nanosheets also have the similar property of absorbing the dye labelled single-stranded DNA much more strongly than double-stranded DNA. Presumably, it is may be that ssDNA was absorbed on the surface of WS₂ nanosheet via the van der waals force between the nucleobases and the plane of WS₂. However, the nucleobases of dsDNA were embedded in the densely negatively charged helical phosphate backbones, so the interaction between dsDNA and WS₂ is very weak.

Here we report a simple but universal WS₂ nanosheets platform using T4 PNKP as a model for analysis of DNA 3'-phosphatase activity and its inhibition by the FRET between dye labelled DNA and WS₂ nanosheets. As far as we know, this is the first time that DNA 3'-phosphatase has been detected using WS₂ nanosheets. The proposed method is simple, economical and convenient. In addition, the proposed method was able to quantitatively investigate the inhibition effect of inhibitors on DNA 3'-phosphatase. Sensitive detection of T4 PNKP activity and inhibitor screening were achieved due to the excellent fluorescence quenching ability of WS₂ nanosheets.



Scheme 1. Schematic representation of WS₂ nanosheets-based platform for T4 PNKP activity and inhibition analysis.

The protocol utilized a dye labelled DNA probe acting as the substrate for T4 PNKP. The probe is a single-strand DNA molecule that forms self-complementary structure at one end. The 3'-end is modified with a phosphate group and serves as the substrate of the target phosphatases. Upon the addition of T4 PNKP, the 3'-phosphoryl of the probe is hydrolyzed to a hydroxyl group and the resulting 3'-hydroxyl is immediately extended by the DNA polymerase and dNTPs. Because of the weak affinity between the double-strand DNA and WS₂ nanosheets, the double-strand product of the elongation reaction showed a great fluorescence emission in the presence of WS₂ nanosheets. Quite low fluorescence signal was observed for the probe without polymerase elongation, and fluorescence was quenched resulting from the interaction between dye labelled single-strand and WS₂ nanosheets. Compared to the traditional methods, the proposed strategy is convenient and exhibiting high analytical performance.

The method is used as an effective approach for the measurement of the activity of T4 PNKP and the inhibition effects of heparin on T4 PNKP. It has been successfully applied to quantify the phosphatase activity in the extract of Hela cell and shows great potential in analysis of phosphatases in other biological samples without any complex pretreatment procedures.

Experimental Section

Chemicals and Materials

The DNA sequences used in this work were synthesized by Shanghai Sangon Biological Engineering Technology & Services Co., Ltd. The sequence of the DNA oligonucleotide is as follows, where the loop sequence is indicated in italics, and complementary sequences are underlined:

Probe1 (P1): FAM- 5'-TAG AGA GAG AGA GAG AGA GAG AGC GCA CCT AAA *GGG TGC G*-phos-3'

Tungsten Disulfide (WS₂) nanosheet was purchased from Nanjing XFNano Material Tech Co., Ltd. (Nanjing, China) and were prepared according to the method reported by Voiry *et al.*²⁶ Briefly, five milliliters of aqueous solution of WS₂ was sonicated in ice bath for 1 h under the power of ~ 3W using a probe-type sonicator. The resulting suspension was centrifuged at 6000g for 30 min to remove possible WS₂ aggregates and then was stored in 4 °C for further usage. T4 polynucleotide kinase phosphatase, Klenow fragment polymerase (KF polymerase, without 3' to 5' exonuclease activity), deoxyribonucleoside triphosphates (dNTPs), apurinic/apyrimidinic endonuclease I (APE I), cAMP-dependent protein kinase (PKA), Casein kinase (CKII) and Uracil-DNA Glycosylase (UDG) were obtained from New England Biolabs (Ipswich, MA, USA). The buffer solutions employed in this work were the following: the reaction buffer was 10 mM Tris-HCl, 10 mM MgCl₂, 50 mM NaCl, and 1 mM DTT (pH 7.9); the detection buffer was 10 mM Tris-HCl, 100 mM NaCl, and 5 mM MgCl₂ (pH 8.0). All reagents were used as received without further purification. All solutions were prepared using ultrapure water, obtained through a Millipore Milli-Q water purification system (Billerica, MA, USA) having an electric resistance >18.3 MΩ.

The fluorescence measurements were carried out on an FL-7000 spectrometer (Hitachi, Japan). The fluorescence emission spectra were collected from 500 nm to 600 nm at room temperature with a 488 nm excitation wavelength.

Assay Procedures

Briefly, a total volume of 25 μL solution containing varying concentrations of T4 PNKP, P1 (50 nM), KF polymerase (100 U/mL), and dNTPs (50 mM) was incubated at 37 °C for 80 min. Then, 10 μL WS₂ (0.025 mg/mL) and the detection buffer were added to give a final volume of 100 μL. After 10 min, the fluorescence of the mixture was measured at 520 nm with the excitation of 488 nm at room temperature.

Kinase Inhibitor Evaluation

T4 PNKP (100 U/mL) was firstly mixed with varying concentrations of heparin, then P1, KF polymerase, dNTPs and reaction buffer were added to give a final reaction volume of 25 mL, and the solution was kept at 37 °C for 80 min. Fluorescence detection was performed at room temperature with the addition of

WS₂ in the same way as for the assay of T4 PNKP.

T4 PNK Activity Detection in Diluted Cell Extracts.

Hela Cells were cultured in RPMI 1640 medium supplemented with 12% fetal calf serum, 100 μg mL⁻¹ streptomycin, and 100 units mL⁻¹ penicillin. Cell extracts were prepared according to the previous reports.²⁷ The collected cells were resuspended in 20 μL 10 mM Tris-HCl (pH 7.8) containing 150 mM NaCl. Into the suspension equal volume of lysis buffer was added which contained 10 mM Tris-HCl (pH 7.8), 150 mM NaCl, 2 mM EDTA, 2 mM DTT, 40% glycerol, 0.2% NP40, and 0.4 mM phenylmethylsulfonyl fluoride. The mixture were incubated for 1.5 h at 4 °C with occasional shake. Cell debris was removed by centrifugation at 10000 rpm for 10 min, and the supernatant was recovered. Diluted cell extracts were added to the assay solution (1%). The detection procedure was the same as those described in the aforementioned experiment for T4 PNKP detection in clean reaction buffer.

Results and discussion

Strategy for T4 PNKP Activity Detection

The proposed strategy for the label-free assay of T4 PNKP and its inhibitor relies on the fact that different adsorption abilities of single-strand DNA and FAM labelled double-strand polymerase elongation product on the WS₂ nanosheet surface could lead to significant discrepancy of the fluorescence signals. The principal design is illustrated in Scheme 1. The primer probe contains two short single stranded complementary sequences which can form a hairpin structure with a 3'-phosphoryl end under appropriate hybridizing conditions. Because the polymerase elongation reaction is only initiated at the 3'-hydroxyl end of the primer, the 3'-phosphorylated DNA probe formed in such a way is an inactive substrate for DNA polymerase in the absence of T4 PNKP, and thus cannot trigger the polymerase elongation. With the addition of WS₂ nanosheets, the fluorescence is greatly quenched, giving a weak background for the sensing system. However, the primer probe can be dephosphorylated into a 3'-hydroxyl end by T4 PNKP, which then can serve as the preferred substrate for DNA polymerase. Therefore, in the presence of T4 PNKP, together with the DNA polymerase and dNTPs, polymerase elongation is initiated to generate a long double-strand DNA product. Because of the weak affinity between the double-strand DNA and WS₂ nanosheets, significant fluorescence quenching will not occur for the elongation product, leading to a strong fluorescence signal after the addition of WS₂ nanosheets. Thus the activity of T4 PNKP can be easily reflected by the fluorescence signal change.

Characterization of WS₂ Nanosheets

WS₂ nanosheets prepared according to the method reported by Voiry et al²⁶ were characterized by transmission electron microscopy (TEM), atomic force microscopy (AFM), and X-ray diffraction (XRD). AFM characterization of the as-prepared WS₂ nanosheets indicated that the thickness of the nanosheets was ~1.2 nm, evidencing the successful synthesis of the one-layer WS₂ nanosheets (Fig. 1). A negative ζ potential of -21.2 mV was observed for the nanosheets (Fig. S1 in ESI), indicating a negative charge on the WS₂ nanosheet surfaces. XRD patterns

revealed that there was no (002) reflection for the nanosheets (Fig. S2A in ESI). Stable dispersions of WS₂ nanosheets were obtained in aqueous solutions, no sediment observed even after the WS₂ nanosheets were stored for more than one week (Fig. S2B in ESI).

Monitoring of the T4 PNK-Catalyzed Dephosphorylation

To verify that the increase of fluorescence signal was indeed caused by the different adsorption abilities of FAM labelled single-strand DNA and double-strand polymerase elongation DNA product. The polymerase elongation was initiated by dephosphorylating DNA probe using T4 PNKP, a proof of principle experiment was carried out in the absence of T4 PNKP or in the presence of inactivated T4 PNKP. As shown in Fig. 2, in the absence of T4 PNKP, the polymerase elongation is not induced and as a result rather weak fluorescence signals were obtained (curves a). Two similarly weak fluorescence signals were also observed in the presence or absence of inactivated T4 PNKP (curves b and c). These fluorescence background signals originated from the strong adsorption of single-strand DNA on WS₂ nanosheets surface and the effective FRET between the dye and WS₂ nanosheets. In the presence of T4 PNKP (100 U/mL), stronger fluorescence signal was observed with a signal-to-background ratio of more than 10 times (curves d), implying the formation of the long double-strand elongation product. These experimental results demonstrated the feasibility of the proposed strategy for the detection of DNA 3'-phosphatase.

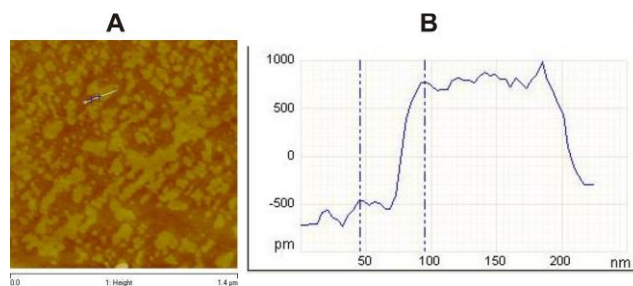
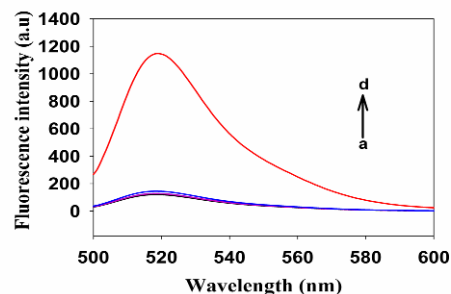


Fig. 1. Typical AFM image of the prepared WS₂ nanosheets.



Typical fluorescence spectra of 50 nM P1 under different conditions: (a) without T4 PNKP dephosphorylation after addition of 10 μL of WS₂ nanosheets in the reaction buffer; (b) without inactivated T4 PNKP after the addition of 10 μL of WS₂ nanosheets in the reaction buffer; (c) with inactivated T4 PNKP after the addition of 10 μL of WS₂ nanosheets in the reaction buffer; (d) with T4 PNKP dephosphorylation after the addition of 10 μL of WS₂ nanosheets in the reaction buffer. The concentrations of T4 PNK and dNTPs were 10 U mL⁻¹ and 50 μM, respectively.

Optimization of Assay Conditions

It was found that the amount of WS₂ nanosheets used has a large influence on the fluorescence quenching. The fluorescence of six samples was measured in the presence of 0, 0.5, 1, 2, 3 and 5 μg mL⁻¹ WS₂ nanosheets, respectively (Fig. S3 in ESI). The increased amount of WS₂ nanosheets leads to an increase in quenching efficiency and a decrease in fluorescence maintenance. Such observations can be explained by following reasoning. When P1 was mixed with WS₂ nanosheets, it adsorb onto the WS₂ nanosheet surface. It is obvious that the use of more WS₂ nanosheets leads to more efficient adsorption of P1, increasing the quenching efficiency. These results indicated that when concentration of WS₂ nanosheets was 3 μg mL⁻¹, the fluorescence intensities of FAM labelled double-strand elongation product relative to the fluorescence intensities of FAM labelled single-strand DNA reached the maximal value. As a result, 3 μg mL⁻¹ was used as the optimized concentration for WS₂ nanosheets.

The concentration of P1 is a crucial parameter for the dephosphorylation process and the polymerase elongation. In order to optimize the P1 concentration, the concentration of DNA 3'-phosphatase was kept constant and we compared the signal-to-background ratio of varying concentrations of P1 with their optimal WS₂ nanosheets usage. As shown in Fig. S4 in ESI, F1/F0 reached a maximum at 50 nM of P1, and decreased gradually along with the P1 concentration up to 125 nM. Thus, the optimal concentration of P1 for assaying T4 PNKP was chosen to be 50 nM, and was used throughout subsequent experiments. Moreover, to achieve the best sensing performance, the reaction time and the concentrations of KF polymerase and dNTPs were also optimized (Fig. S5 in ESI); experimental results showed that the following conditions provided the maximum S/N ratio for the sensing system: 50 nM P1, 100 U mL⁻¹ KF polymerase, 50 mM dNTPs and a reaction time of 80 min for T4 PNKP.

Fluorescence Measurement of T4 PNKP Activity

We choose the fluorescence emission at 520 nm to evaluate the performances of the proposed method. The activity of T4 PNKP was quantified based on the optimal experimental conditions. Fig. 3A depicted the typical fluorescence spectral responses of the fluorescent biosensor to T4 PNKP at varying concentrations. We observed that dynamically increased fluorescence peaks with increasing T4 PNKP concentration ranging from 0.1 to 100 U mL⁻¹. Fig. 3B indicated the fluorescence signal was linearly decreased with the T4 PNKP concentration in the range from 0.1 to 100 U mL⁻¹ (regression coefficient $R^2 = 0.995$). The proposed method also showed good reproducibility, the relative standard deviations of peak fluorescence readings were 3.4%, 2.8%, 1.5% and 2.5% in three repetitive assays of 0.1 U mL⁻¹, 1 U mL⁻¹, 10 U mL⁻¹ and 100 U mL⁻¹ T4 PNKP, respectively. The detection limit was estimated to be 0.05 U mL⁻¹ according to the 3σ rule, which was much lower than the previously reported fluorescent assay based on a universal molecular beacon and quantitative real-time PCR,²⁸ and comparable to another fluorescent assay based on a coupled exonuclease reaction and a graphene oxide platform.²⁹ The results demonstrated that the proposed method could be used as a highly sensitive fluorescent biosensor for T4 PNKP detection

Assay Selectivity

To demonstrate the selectivity of the present strategy, control experiments using some nonspecific enzymes including CKII, PDGF-BB, APE 1, UDG and PKA were respectively tested with the procedures of T4 PNKP assay and the same concentration of T4 PNKP (100 U mL⁻¹). With the comparison of peak intensity after treatment by these enzymes, it was obviously observed that these nonspecific enzymes did not cause a remarkable fluorescence increase, indicating a high selectivity of the proposed WS₂ nanosheets-based T4 PNKP assay (Fig. 4).

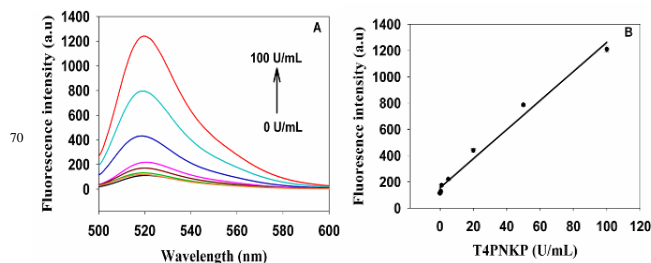


Fig. 3. (A) Fluorescence intensity_wavelength curves with different activity units of T4 PNKP (bottom to top, 0, 0.1, 0.5, 1, 5, 20, 50, 100 U mL⁻¹) in reaction buffer. (B) Calibration curve of WS₂ nanosheets nanosensor in the presence of increasing amount of T4 PNKP dependence of fluorescence intensity on T4 PNKP concentration. The concentration of P1 was 50 nM. The error bars represented for standard deviation (SD) across three repetitive experiments.

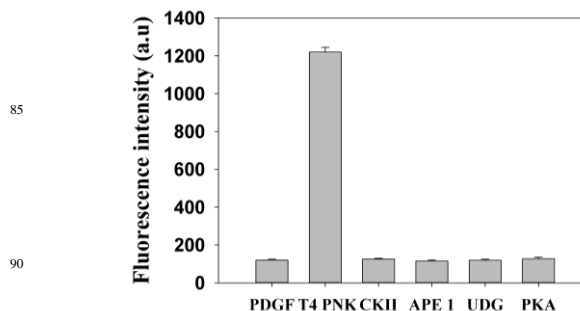


Fig. 4. The selectivity of the WS₂ nanosheets-based strategy for T4 PNKP assay. The concentrations of all enzymes were 100U mL⁻¹. Error bars were estimated from three replicate measurements. (P1 50 nM, KF polymerase 100U mL⁻¹, dNTPs 50 mM, WS₂ 3 μg mL⁻¹).

Investigation of T4 PNKP Activity Detection in Diluted Cell Extracts

The feasibility of the proposed strategy was also tested by the detection of T4 PNKP in complex biological samples. In order to examine the possibility of the as-proposed sensing platform for cellular T4 PNKP activity profiling, HeLa cell extracts were added in the buffer to simulate the intracellular environment during the test procedure. WS₂ nanosheets were found well dispersed in the reaction buffer containing 1% (v/v) cell extracts and no sediment was observed after 48 h. It was observed from Fig. S6A in ESI that the fluorescence signals decreased when the concentrations of T4 PNKP gradually increased from 0.1 to 100 U mL⁻¹. The fluorescence intensity and the logarithm of T4 PNKP concentration also exhibited a linear relationship like that operated in Tris-HCl buffer (Fig. S6B). The above results demonstrated that the as-proposed sensing platform works well in complex mixtures with other possible coexisting interfering species, suggesting that the method could be further used for real

sample analysis.

Assay of the Inhibition on T4 PNKP Activity

The established strategy can be further adapted to study the effects of inhibitor compounds on the phosphatase activities of T4 PNKP. Heparin has been reported to be inhibitors of T4 PNKP. Furthermore, the activity of KF polymerase was not affected by the inhibitor compounds under the experimental conditions (data not shown). Fig. 5 shows the effect of heparin on the activity of T4 PNKP. As the heparin concentration increased, the relative activity of T4 PNKP decreased sharply. The half-maximal inhibitory concentration (IC_{50}) of heparin was acquired from the plot of relative activity of T4 PNKP versus heparin concentration and was found to be 0.16 mg mL^{-1} . As demonstrated by the above experimental results, the inhibition effect of the inhibitor compounds on the phosphatase activities of T4 PNKP could also be quantitatively evaluated, the proposed method could be also readily applied to assay other DNA 3'-phosphatases.

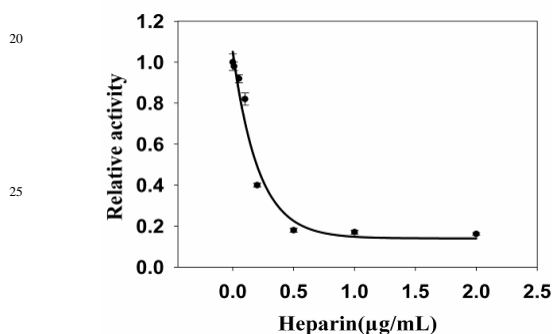


Fig. 5. Inhibition effects of heparin on dephosphorylation. The concentration of T4 PNKP is 100 U mL^{-1} . The concentrations of heparin are 0, 0.02, 0.05, 0.1, 0.2, 0.5, 1.0 and 2.0 mg mL^{-1} , respectively. The error bars represented for standard deviation (SD) across three repetitive experiments.

Conclusion

In conclusion, a novel highly sensitive WS_2 nanosheets-based sensing platform for the assay of DNA 3'-phosphatases T4 PNKP and its inhibitors was developed based on a single-strand DNA molecule that forms self-complementary structure at one end and polymerase elongation. The assay relies on the principle that the polymerase elongation reaction is only initiated at the 3'-hydroxyl end of the probe, and the absorption of FAM labelled double-stranded of elongation product at the WS_2 nanosheet surface is weak and unstable. The proposed strategy is simple and convenient, showing high sensitivity and selectivity, due to the super quenching ability of WS_2 nanosheets. Our method was also used to investigate the effects of inhibitor compounds on the phosphatase activities of DNA 3'-phosphatases and satisfactory results were obtained. In addition, the proposed strategy was applicable to a real biological sample. Given the simplicity, selectivity and sensitivity of this method, the proposed strategy may become a method of choice for the assay of DNA 3'-phosphatases and will find application in the study of DNA damage repair mechanisms.

Acknowledgement

This work was supported by the National Natural Science Foundation of China (No. 21275045), NCET-11-0121, Hunan Provincial Natural Science Foundation of China (Grant 12JJ1004) and Fundamental Research Funds for the Central University (No.531107040687).

Notes and references

- State Key Laboratory for Chemo/Biosensing and Chemometrics, College of Chemistry and Chemical Engineering, Hunan University, Changsha, 410082, P. R. China. el.: 86-731-8822577; fax: 86-731-8822782; E-mail addresses: rquy@hnu.edu.cn (R.-Q. Yu).
- W. D. Henner, L. O. Rodriguez, S. M. Hecht, and W. A. Haseltine, *J. Biol. Chem.*, 1983, **258**, 711–713.
 - B. N. Ames, L. S. Gold, and W. C. Willett, *Proc. Natl. Acad. Sci. U. S. A.*, 1995, **92**, 5258–5265.
 - F. Karimi-Busheri, J. Lee, A. E. Tomkinson, and M. Weinfeld, *Nucleic Acid Res.*, 1998, **26**, 4395–4400.
 - W. D. Henner, S. M. Grunberg, and W. A. Haseltine, *J. Biol. Chem.*, 1983, **258**, 15198–15205.
 - S. W. Yang, A. B. Jr. Burgin, B. N. Huizenga, C. A. Robertson, K. C. Yao, and H. A. Nash, *Proc. Natl. Acad. Sci. U. S. A.*, 1996, **93**, 11534–11539.
 - C. C. Richards, *Proc. Natl. Acad. Sci. U.S.A.*, 1965, **54**, 158–165.
 - D. H. Phillips, and V. M. Arlt, *Nat. Protoc.*, 2007, **2**, 2772–2781.
 - C. Frauendorf, F. Hausch, I. Rohl, A. Lichte, S. Vonhoff, and S. Klussmann, *Nucleic Acids Res.*, 2003, **31**, e34.
 - F. Karimi-Busheri, A. Rasouli-Nia, J. Allalunis-Turner, and M. Weinfeld, *Cancer Res.*, 2007, **67**, 6619–6625.
 - L. K. Wang, C. D. Lima, and S. Shuman, *EMBO J.*, 2002, **21**, 3873–3880.
 - F. Karimi-Busheri, J. Lee, A. E. Tomkinson, and M. Weinfeld, *Nucleic Acids Res.*, 1998, **26**, 4395–4400.
 - A. Jilani, D. Ramotar, C. Slack, C. Ong, X. M. Yang, S. W. Scherer, and D. D. Lasko, *J. Biol. Chem.*, 1999, **274**, 24176–24186.
 - L. K. Wang, and S. Shuman, *J. Biol. Chem.*, 2001, **276**, 26868–26874.
 - A. Rasouli-Nia, F. Karimi-Busheri, and M. Weinfeld, *Proc. Natl. Acad. Sci. U. S. A.*, 2004, **101**, 6905–6910.
 - C. B. Ma, Z. W. Tang, K. M. Wang, W. H. Tan, X. H. Yang, W. Li, Z. H. Li, Li, H. M. Li, and X. Y. Lv, *Chembiochem.*, 2007, **8**, 1487–1490.
 - X. Huang, X. Y. Qi, F. Boey, and H. Zhang, *Chem. Soc. Rev.*, 2012, **41**, 666–686.
 - Y. Wang, Z. H. Li, D. H. Hu, C. T. Lin, J. H. Li, and Y. H. Lin, *J. Am. Chem. Soc.*, 2010, **132**, 9274–9276.
 - L. H. Tang, Y. Wang, Y. Liu, and J. H. Li, *ACS Nano*, 2011, **5**, 3817–3822.
 - B. W. Liu, Z. Y. Sun, X. Zhang, and J. W. Liu, *Anal. Chem.*, 2013, **85**, 7987–7993.
 - C. H. Lu, H. H. Yang, C. L. Zhu, X. Chen, and G. N. Chen, *Angew. Chem., Int. Ed.*, 2009, **48**, 4785–4787.
 - Y. S. Guo, X. P. Jia, and S. S. Zhang, *Chem. Commun.*, 2011, **47**, 725–727.
 - W. J. Zhao, Z. Ghorannevis, L. Q. Chu, M. L. Toh, C. Kloc, P. H. Tan, and G. Eda, *ACS Nano*, 2013, **7**, 791–797.
 - M. Bernardi, M. Palumbo, and J. C. Grossman, *Nano Lett.*, 2013, **13**, 3664–3670.
 - J. W. Liu, and Y. Lu, *J. Am. Chem. Soc.*, 2007, **129**, 9838–9839.
 - S. J. He, B. Song, D. Li, C. F. Zhu, W. P. Qi, Y. Q. Wen, L. H. Wang, S. P. Song, H. P. Fang, and C. H. Fan, *Adv. Funct. Mater.*, 2010, **20**, 453–459.
 - D. Voiry, H. Yamaguchi, J. W. Li, R. Silva, D. C. Alves, T. Fujita, M. W. Chen, T. Asefa, V. B. Shenoy, G. Eda, and M. Chhowalla, *Nat. Mater.*, 2013, **12**, 850–855.
 - M. D. Vodenicharov, F. R. Sallmann, M. S. Satoh, and G. G. Poirier, *Nucleic Acids Res.*, 2000, **28**, 3887–3896.
 - C. Song, C. Zhang, and M. P. Zhao, *Chem. Asian J.*, 2010, **5**, 1146–1151.
 - L. Lin, Y. Liu, X. Zhao, and J. H. Li, *Anal. Chem.*, 2011, **83**, 8396–8402.